

Adsorbate-induced shifts of electronic surface states: Cs on the (100) faces of tungsten, molybdenum, and tantalum

P. Soukiassian,* R. Riwan, and J. Lecante

*Service de Physique des Atomes et des Surfaces, Centre d'Etudes Nucléaires de Saclay,
F-91191 Gif-sur-Yvette Cédex, France*

*and Laboratoire d'Utilisation du Rayonnement Electromagnétique (LURE), Université de Paris—Sud,
F-91405 Orsay Cédex, France*

E. Wimmer,† S. R. Chubb, and A. J. Freeman‡

Materials Research Center and Department of Physics and Astronomy, Northwestern University, Evanston, Illinois 60201

(Received 30 July 1984; revised manuscript received 13 November 1984)

The adsorption of cesium on the (100) faces of W, Mo, and Ta for coverages between 0 and 1 monolayer is studied by angle-resolved ultraviolet photoemission spectroscopy with use of synchrotron radiation, by electron-energy-loss spectroscopy, and by low-energy electron diffraction. With increasing cesiation, the W(100) surface state at $\bar{\Gamma}$ located 0.3 eV below the Fermi level is shifted by up to 1.0 eV to larger binding energies while remaining sharp and intense. A similar behavior is observed on Ta(100), whereas on Mo(100) the shift of 0.9 eV of this surface state is accompanied by a pronounced attenuation of its intensity. These experimental shifts are shown to be in excellent agreement with all-electron local-density-functional results obtained with the full-potential linearized augmented-plane-wave method for Cs monolayers on the W(100) and Mo(100) surfaces. Based on these *ab initio* results, the electronic origin of the shifts is understood by the formation of strongly polarized covalent bonds between the *d*-like surface states and the Cs 6*s*-derived valence states. It is argued that even at high Cs coverages, the main electron-energy-loss peaks, which are observed between 1 and 2 eV, could be interpreted as Cs 6*s*→6*p*-like interband transitions rather than as surface-plasmon peaks.

I. INTRODUCTION

Electronic surface states (SS's) are well known to be sensitive to adsorbates; in many cases such as oxygen adsorbed on Mo(100) (Ref. 1) and W(100) (Ref. 2) or hydrogen on W(100) (Ref. 3) the SS's of the substrate are readily destroyed by the adsorbate. Only in exceptional cases has the response to adsorption been observed to be different: very high exposures of the (100) face of Mo (Ref. 4) to H₂ cause an attenuation of the SS photoemission peaks without any displacement of their energies. On the other hand, Hg adsorbed on the W(100) surface has been found⁵ to leave the SS's of the substrate unaffected. Similarly, layer growth of Au and Cu studied with field emission energy distribution (FEED) measurements by Billington and Rhodin⁶ showed the appearance of SS's of the W substrate with completed one and two monolayer coverages. However, between these coverages the SS could not be detected. Recently, Lindgren and Wallden⁷⁻⁹ studied the effect of Cs adsorption on the *s,p*-like SS on Cu(111) at normal emission angle and found that this state located at 0.4 eV below the Fermi level was shifted by 0.4 eV to larger binding energies with considerable attenuation. Adsorption of oxygen caused a shift of this SS to smaller binding energies^{9,10} and CO adsorption lead to a shift to smaller binding energies together with a rapid decrease in intensity of the photoemission peak associated with this SS.¹¹ In this context, the study of alkali adsorption on transition metal surfaces such as W(100), Mo(100), and Ta(100) is of par-

ticular interest since the understanding of their crystallographic and electronic structures still presents challenging scientific problems.

In this paper, we present a combined experimental and theoretical investigation of the effect of Cs adsorption on the SS's of the (100) faces of Mo, W, and Ta as observed by angle-resolved ultraviolet photoemission spectroscopy (ARUPS) at normal emission. The photoemission data,¹² obtained by using synchrotron radiation, are augmented by¹³ electron energy loss spectroscopy (EELS) and low-energy electron diffraction (LEED) measurements.^{14,15} These experimental results are discussed in the light of fully self-consistent all-electron local-density functional (LDF) calculations performed for monolayers of Cs on W(100) and Mo(100) (Refs. 16 and 17, respectively) surfaces. Upon adsorption of Cs on the (100) surfaces of W, Mo, and Ta, the SS's located at $\bar{\Gamma}$ just below the Fermi level are shifted by about 1 eV to larger binding energies. All-electron LDF calculations for the systems Cs/W(100) and Cs/Mo(100) quantitatively describe these adsorbate induced shifts of the SS's and reveal their electronic origin: the SS's, which have *d*_{z²}-like character and project far out into the vacuum, form polarized covalent bonds with the Cs 6*s*-derived states. Consequently, the energy of the hybridized bonding state is lower than that of the SS on the clean surface while its charge distribution near the surface *d*-metal atom remains essentially unaltered. Furthermore, EELS data obtained for cesiated W(100) and Mo(100) surfaces show a characteristic loss peak

which is shifted to smaller energies upon cesiation. The present theoretical results provide evidence that these energy losses can be interpreted^{12,13} as Cs $6s \rightarrow 6p$ -like interband transitions, rather than as surface plasmons.

II. BACKGROUND PERSPECTIVE

The crystallographic structures of alkali overlayers on metallic substrates as a function of coverage, the corresponding work function changes, and adsorption energies have been studied for a variety of systems using mainly low-energy electron diffraction (LEED), contact potential, and thermal desorption methods. From these studies, a consistent picture has emerged: upon alkali adsorption, the work function of the substrate drops rapidly, reaches a minimum, and then increases slightly to a plateau at coverages greater than a monolayer. At full monolayer coverage the alkali atoms form close-packed hexagonal structures as has been observed for Cs/W(100),¹⁸ Cs/W(110),¹⁹ K/Ni(100),²⁰ K/Pt(111),²¹ Na/Al(100) and Na/Al(111),²² Cs/Cu(111),²³ Cs/Cu(100),²⁴ and Cs/Ir(100).²⁵ At lower coverages, ordered overlayer structures have been observed for systems such as $p(2 \times 2)$ Cs/W(100),¹⁸ $c(2 \times 2)$ Na/Ni(100),²⁶ and $c(2 \times 2)$ Na/Al(100).²² In other cases, e.g., Cs/W(110) (Ref. 19) and K/Ni(100),²⁰ the adsorbate atoms are uniformly spread and their interatomic distances decrease continuously with increasing coverage. Furthermore, adsorbed alkali atoms have been found to induce a reconstruction of the substrate such as the (110) faces of Ag and Cu (Ref. 27) and the (100) faces of Mo and W.¹⁴ In general, the desorption energy per atom has been found to decrease with increasing coverage.

The electronic structure of the alkali atoms adsorbed on transition-metal surfaces has been explored mainly by using electron-energy-loss spectroscopy (EELS), Auger electron spectroscopy (AES), work-function measurements and, in some cases ultraviolet photoemission spectroscopy (UPS). Changes in energy loss with the coverage of alkalis on Ni(100) (Refs. 28–30) and on Cu(111) (Refs. 7 and 31) have been attributed to collective oscillations of a free-electron gas in the overlayer of varying density. The same mechanism was first proposed by MacRae *et al.* for Cs on W(100) (Ref. 32) and by Thomas and Haas³³ for Rb on the same substrate. Theoretical studies by Gadzuk,³⁴ Ghai *et al.*,³⁵ and Newns³⁶ have provided a justification for interpreting these excitations in the submonolayer coverage as surface plasmons and these authors have calculated theoretical dispersion curves on this basis. The observation of the occupied $6s$ resonance for Cs on Cu(111) above a half-monolayer coverage in ARUPS^{7,31} has provided further confirmation of the validity of this model (assumed to be applicable for all substrates).

However, interband transitions are well known as another mechanism for electron energy losses. This fact has been used to interpret the EELS results for low coverages of Na, K, and Rb overlayers on Ni(100),^{28,29,37} Na on Pt(111),³⁸ and for Na and Cs on Cu(111).³¹ Generally, these authors consider transitions from occupied valence states into unoccupied adsorbate states. Recent EELS and ARUPS experiments^{12,13} for Cs adsorbed on W(100), Mo(100), and Ta(100) provided further indications that

the interactions between adsorbed alkali atoms and transition-metal substrates cannot be explained satisfactorily by a simple theoretical model which ignores the detailed electronic structure due to the presence of d electrons at the surface.

The small ionization potentials of the alkali atoms and the rather large work functions of clean transition-metal surfaces suggest that the adsorbed alkali atoms are largely ionic or strongly polarized at low coverages. This is evident from the initial rapid decrease of the work function upon alkali deposition observed for a variety of systems^{13,18,19,22,31,39–42} and has been further demonstrated by core level shifts, e.g., for the system K/Fe(110).⁴⁰ At high coverages, metallic overlayers have been assumed, e.g., for K/Ag(111).⁴¹

This wealth of experimental data for alkali overlayers on metallic substrates has spawned a fascinating field for theoretical efforts to describe the interaction between adsorbate and substrate. We recall briefly the main existing approaches to alkali adsorption on metals. The first model was given by Langmuir^{43,44} who assumed that at low coverages the alkali atoms are adsorbed as ions with their valence electrons being transferred to the metal substrate. The positive ions together with their negative image charges form dipoles which lower the work function. At higher coverages, dipole-dipole interactions lead to a depolarization⁴⁵ and further to a minimum in the work function. Beyond this minimum, neutralization of the ions is achieved. As illustrated recently by Desplat and Papageorgopoulos,⁴⁶ this assumption seems to be supported by the fact that Cs atoms desorb as positive ions at low coverages and as neutral atoms at high coverages. Another model given by Levine and Gyftopoulos⁴⁷ considers the surface as a dipole barrier and an electronegative barrier. The charge transfer in this theory is proportional to the electronegativity difference between the surface and the adsorbate. The adsorbate is essentially ionic at low coverages and covalent beyond the half-monolayer up to the monolayer coverage.

Various quantum-mechanical approaches have been attempted to describe the interaction between the adsorbate and the substrate. In the first step, a simplified Hamiltonian^{48–50} or a modified Anderson Hamiltonian^{51–54} have been introduced assuming a weak adatom-metal interaction associated with extended wave functions. Localized surface states are excluded,⁴⁹ so that perturbation methods may be used. Muscat and Newns⁵¹ justify the extrapolation of their results obtained for alkali adsorption on free-electron (s,p) metals to transition-metal substrates by assuming that the Cs- $6s$ interaction with d electrons is negligible. [They observe that (i) the work-function-versus-coverage curves are similar for a great variety of metal substrates and (ii) the energy loss in the Cs monolayer is nearly the same for a variety of transition metals.] Using this approach, Braun *et al.*⁵⁴ obtained a good fit to the experimental work function curves for Cs on W(110) and W(111).

Using the local density functional (LDF) approach,⁵⁵ Lang⁵⁶ considered the substrate as semi-infinite jellium with the proper electron density, the adsorbate being represented by a jellium slab. This model was extended to

crystalline substrates by Khan and Ying⁵⁷ who found evidence for specific adsorption sites for Na on Al(111). Wojciechowski⁵⁸ found that for Cs on W(100), the adsorbate is atomlike near half-monolayer and becomes metallic near the completed monolayer coverage. This approach gives the overall shape of the change in the electron density at the surface, the induced dipole moment and hence the work-function change. For a detailed discussion the reader is referred to recent review articles by Muscat and News⁵⁹ and Schulte and Hölzl.⁶⁰

Clearly, these two approaches, even in their most elaborated forms, only consider the interaction with free-electron metals⁶¹ or the delocalized electrons in transition metals but cannot account for a detailed understanding of localized *d*-like states at the surface known to be so important on transition-metal surfaces.

Recently, Wimmer *et al.*¹⁶ reported the first rigorous, all-electron LDF study of Cs adsorbed on the W(001) surface in a probe of the high-coverage limit. From this study it became evident that the *d*-like surface states of the W(001) surface play an important role in the interaction between the Cs atoms and the transition metal substrate. Significantly, the surface state at $\bar{\Gamma}$, located 0.3 eV below the Fermi surface was found to be shifted by 1.0 eV toward larger binding energy due to the formation of a polarized covalent bond between the (Cs-6*s*)-derived states and the W(*d*) surface state. This shift was reported independently by Soukiassian *et al.*¹² as observed by ARUPS.

III. TECHNICAL ASPECTS

A. Experimental

The measurements were performed in an ultrahigh vacuum chamber with base pressure maintained in the 10^{-11} -Torr range. The experimental setup⁶² provides two levels. The upper level is equipped with a four-grid retarding field analyzer for low-energy electron diffraction (LEED) and Auger measurements, an alkali source, a quadrupole analyzer, and an ion gun. The lower level contains the electron spectrometer with a hemispherical (180°) monochromator and analyzer.⁶³ For the ARUPS experiments, an identical ultrahigh vacuum chamber with a cylindrical photoelectron analyzer is used. The synchrotron radiation emitted by the ACO-LURE (Laboratoire pour l'Utilisation du Rayonnement Electromagnétique émis par les Anneaux de Collisions de l'Accélérateur linéaire d'Orsay) storage ring is focused by a toroidal mirror on a photon monochromator.⁶⁴ The resolution is 150 meV in EELS and ARUPS. The ARUPS experiments are performed with *p* polarization at an incident angle of $\alpha=80^\circ$ and the photoelectrons are collected at normal emission angle. In the EELS experiments the reflected beam is analyzed in the specular direction.

Pure cesium is deposited onto the metal surface after thorough degassing of a resistively heated Cs chromate source in which reduction is achieved by an Al-Zr alloy.⁶⁵ The growth of cesium layers is monitored by LEED and AES measurements.¹⁴

The W(100) and Mo(100) surfaces were cleaned by oxidation cycles (2 h at 10^{-6} Torr of oxygen at 1300 K) and flash heating to 2200 K for tungsten and 1900 K for molybdenum. For the Ta(100) surface, ion bombardment sequences and flashes at 2800 K were used. These sequences were repeated until a clean surface was obtained as characterized by Auger electron spectroscopy (AES).

B. Theoretical/computational

For the theoretical/computational description of the surfaces and overlayers we use the single slab (or thin film) approach which is now well established to reproduce accurately surface electronic structures.⁶⁶ In our calculations,^{16,17} the W and Mo substrate is represented by a film of five atomic layers. Cs overlayers on both sides of this slab are assumed in a $c(2 \times 2)$ overlayer structure with the Cs atoms above fourfold hollow sites of the surface substrate atoms. This (hypothetical) overlayer structure models the situation at completed Cs monolayer coverage. Since no experimental data are available for the height of Cs atoms adsorbed on transition-metal surfaces, we assume for both systems, Cs/W(100) and Cs/Mo(100), the same distance of 2.9 Å between the planes of the surface W (Mo) atoms and the Cs adsorbate. This choice of 2.9 Å was found earlier¹⁶ to give a reasonable value for the work function (which is very sensitive¹⁶ to the assumed height of the Cs atoms) and has been retained in the present study. The electronic structure is calculated from all-electron local-density-functional (LDF) theory.⁵⁵ We use the self-consistent full-potential linearized augmented plane wave (FLAPW) method⁶⁷ for thin films to calculate energy-band structures and charge densities. The main features of this method are (i) all electrons of the system are included in the self-consistency procedure; (ii) the single-particle wave functions for the valence states are expanded in a highly flexible variational basis set; (iii) the core electrons are treated fully relativistically and the valence electrons semirelativistically⁶⁸ (i.e., by dropping the spin-orbit interaction term, but retaining the other relativistic terms in the Hamiltonian); (iv) no shape approximations are made to either the charge density or the potential. Details of the approach have been presented elsewhere.⁶⁷

IV. EXPERIMENTAL RESULTS

A. ARUPS

1. Cs/W(100)

The angle-resolved ultraviolet photoemission spectroscopy (ARUPS) measurements were performed using synchrotron radiation with *p* polarization and normal emission angle. Figure 1 shows the ARUPS results obtained for Cs on W(100) between 0 and 1 monolayer coverage using a photon energy = 78 eV. For convenience we denote with $\Theta=1$ the complete monolayer coverage. With respect to the substrate this corresponds to a coverage of 0.43. The most important feature in the ARUPS spectra concerns the high-lying (HL) tungsten surface state E_1 located near the Fermi level: Upon cesiation, peak E_1

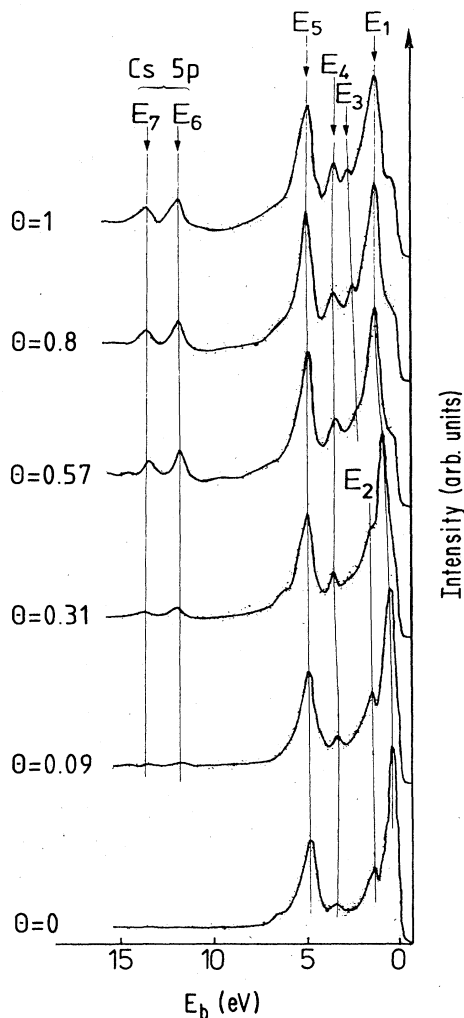


FIG. 1. Cs/W(100). Normal emission angle ARUPS spectra for increasing Cs coverage ($\Theta=1$ corresponds to a completed Cs monolayer) using a photon energy = 78 eV and *p* polarization.

remains sharp and intense up to full monolayer coverage. Its energy exhibits a continuous shift which reaches 1 eV at a coverage of $\Theta=0.6$ monolayer and then remains constant (cf. Figs. 1 and 2). Figure 3 shows ARUPS data obtained for $\Theta=0.8$ monolayer when the photon energy is changed between 50 and 78 eV. As expected for a surface state, the ionization energy does not depend on the incident photon energy. Furthermore, its intensity also remains almost unchanged in this range. As can be seen from Fig. 1, the linewidth of E_1 remains constant up to $\Theta=0.8$ monolayer and a small increase is observed above this coverage due to its overlap with peak E_2 . The bulk peaks E_4 and E_5 (Fig. 1) are not affected by the adsorption. Peaks E_6 and E_7 correspond to the cesium $5p_{3/2}$ and $5p_{1/2}$ semicore levels which, remarkably, keep the same binding energy for all coverages between 0 and 1 monolayer.

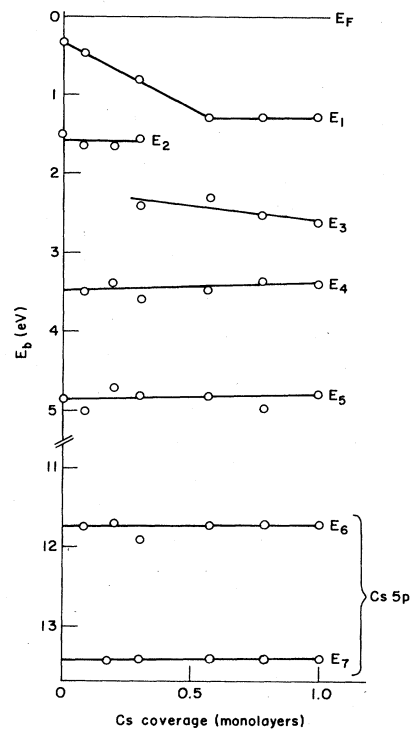


FIG. 2. Cs/W(100). Energy of ARUPS peaks versus cesium coverage Θ .

2. Cs/Ta(100)

The ARUPS data for the system Cs/Ta(100) (Figs. 4 and 5), recorded with a photon energy of 70 eV and *p* polarization, show very similar features compared with the

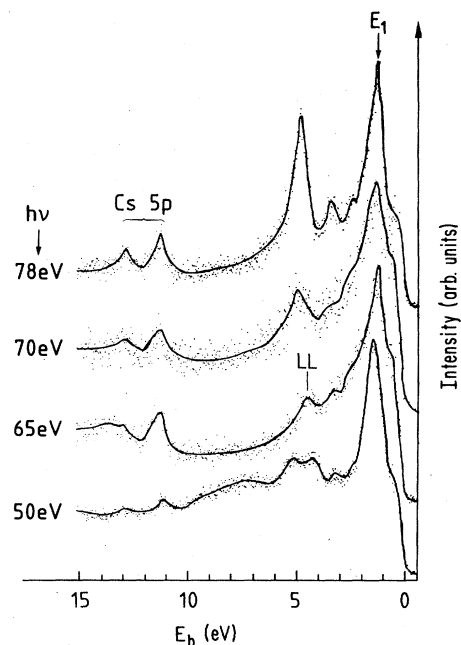


FIG. 3. 0.8 monolayer of Cs/W(100). ARUPS spectra for various photon energies, *p* polarization, and normal-emission angle.

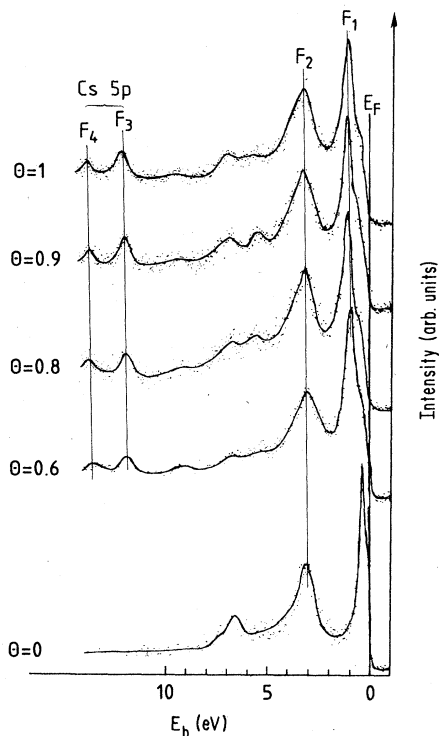


FIG. 4. Cs/Ta(100). ARUPS spectra for increasing Cs coverage Θ , using an incident photon energy = 70 eV, p polarization, and normal-emission angle.

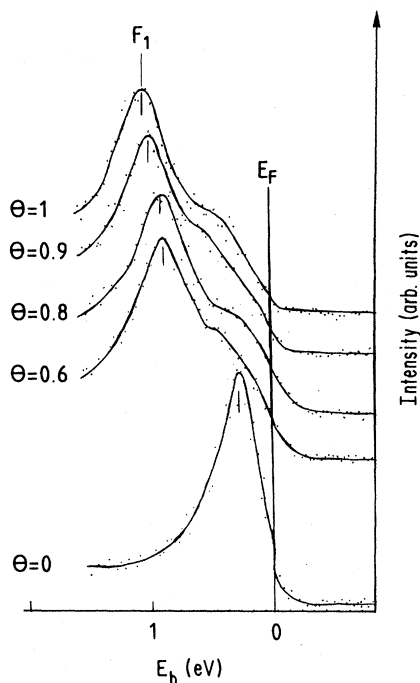


FIG. 5. Cs/Ta(100). ARUPS spectra showing the high-lying Ta(100) surface state at $\bar{\Gamma}$, upon Cs adsorption. A photon energy = 70 eV, p polarization, and normal-emission angle are used.

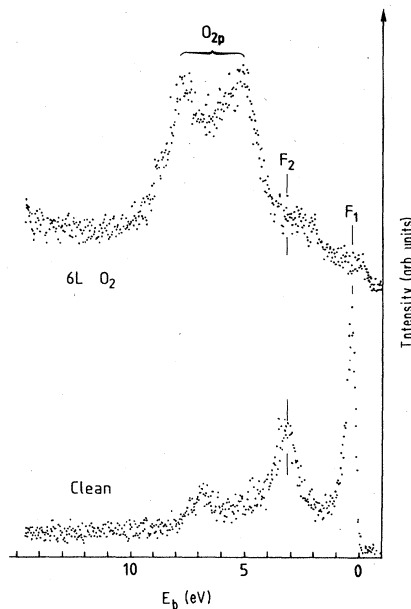


FIG. 6. Cs/Ta(100). ARUPS spectra showing the sensitivity of peaks F_1 and F_2 to an exposure of 6 L of oxygen using a photon energy = 70 eV, p polarization, and normal-emission angle.

Cs/W(100) system: the peak F_1 situated near the Fermi level is shifted to larger binding energies and remains sharp and intense. At completed monolayer coverage, this shift of 0.8 eV is smaller than in the case of W(100). The peak F_2 is not affected by the Cs adsorption (cf. Fig. 4). The sensitivity of the features F_1 and F_2 to deposition of oxygen (cf. Fig. 6) and the fact that this energy shows no dispersion with k_1 (Ref. 69) identifies them as high- and low-lying surface states—in agreement with a recent theoretical investigation.⁷⁰ The peaks F_3 and F_4 originate from the Cs $5p_{3/2}$ and $5p_{1/2}$ semicore states. As was found also for Cs on W(001), the energy position of these $5p$ signals does not significantly change with increasing Cs coverage.

3. Cs/Mo(100)

The photoemission spectra of the Mo(100) surface as a function of increasing Cs coverage recorded at 30 eV exhibit different behavior (Figs. 7 and 8). Upon cesiation, the intensity of the surface state peak just below the Fermi energy is dramatically decreased and broadened while being shifted to larger binding energies. This quenching of the intensity of the Mo surface state by Cs adsorption has been observed in earlier ARUPS results using He (I) radiation.¹³ Furthermore, near and at completed monolayer coverage (cf. Fig. 8), a peak is observed at the original position of the surface state. Using the higher photon energy of 50 eV (Fig. 9), a similar shift and broadening is found. However, at this photon energy, the bulk peak D_2 clouds the situation for coverages greater than 0.5 monolayer (cf. Fig. 9).

Peak D_3 , the low-lying surface state, is slightly affected by the Cs adsorption and appears to be shifted by 300

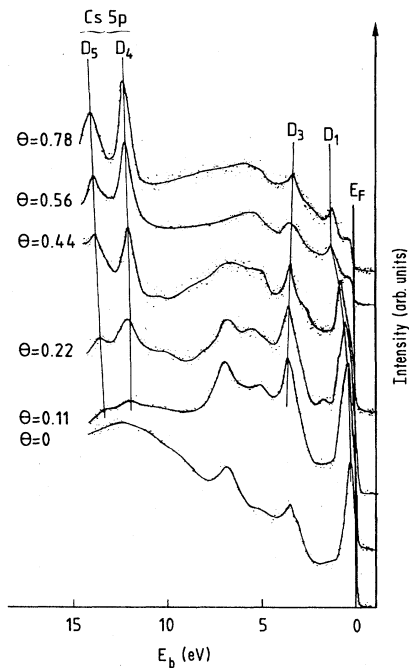


FIG. 7. Cs/Mo(100). ARUPS spectra for increasing Cs coverage using an incident photon energy = 30 eV, p polarization, and normal-emission angle.

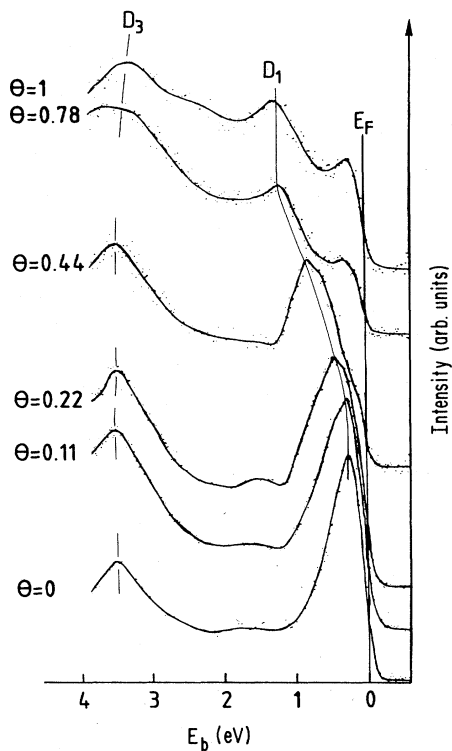


FIG. 8. Cs/Mo(100). ARUPS spectra showing the high-lying and low-lying Mo(100) surface states upon Cs adsorption. A photon energy = 30 eV, p polarization, and normal-emission angle are used.

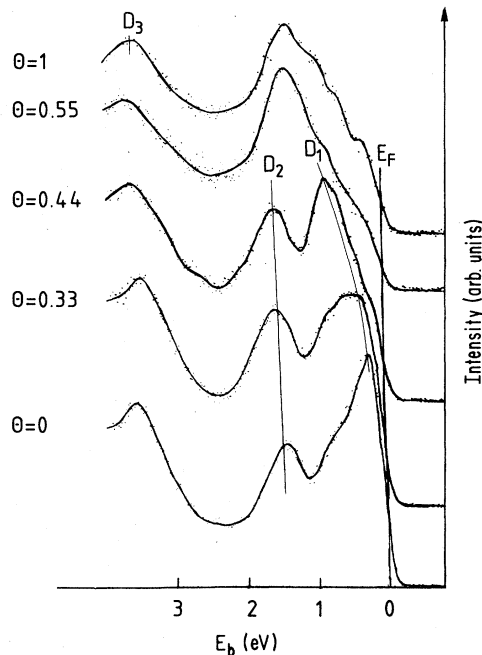


FIG. 9. Cs/Mo(100). ARUPS spectra for increasing Cs coverage using an incident photon energy = 50 eV, p polarization, and normal-emission angle.

meV to smaller binding energies (cf. Figs. 9 and 10). No peak corresponding to E_3 (Fig. 1) is observed for Cs/Mo(100) at these energies.

B. EELS

The main feature in the electron-energy-loss spectra of Cs/W(100) and Cs/Mo(100) (Figs. 11–13) is the energy

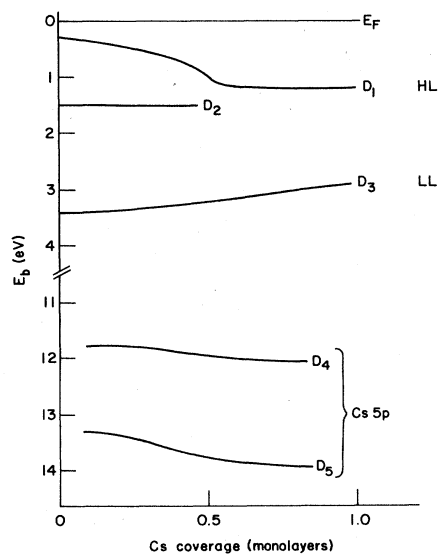


FIG. 10. Cs/Mo(100). Energy of ARUPS peaks D_i versus cesium coverage θ . HL and LL denote the high-lying and the low-lying surface states, respectively.

loss P_1 , which is shifted from 2.9 eV at low cesium coverage to 1.5 eV at half-monolayer coverage for Cs/W(100) and to 1.6 eV for Cs on Mo(100) (cf. Figs. 12 and 13). The shift of the energy loss of these two systems is found to be independent of the energy of the incident beam. On Mo (Fig. 12), the loss peak A (1.4 eV) disappears at low coverages, while on W, the loss peak A' is less sensitive to the adsorption and overlaps with P_1 above a half monolayer.

Additional small features are present on both metals: (i) a peak P_2 is revealed by a peak-separation treatment¹³ (0.8 eV at $\Theta=1$); (ii) P_3 and P_4 with an energy loss of 2.6 and 3.4 eV, respectively; (iii) P_5 and P_6 (Fig. 12), which correspond to transitions from the Cs-5*p* semicore states to an empty state near the Fermi level. On Mo(100), the intensity of the surface plasmon B at 10 eV decreases with increasing cesium coverage¹³ as in the case of oxygen adsorption.^{71,72}

C. LEED

On Mo(100), a $(\sqrt{2} \times \sqrt{2})R45^\circ$ pattern is observed for a Cs coverage of 0.3 (corresponding to 0.13 in terms of the

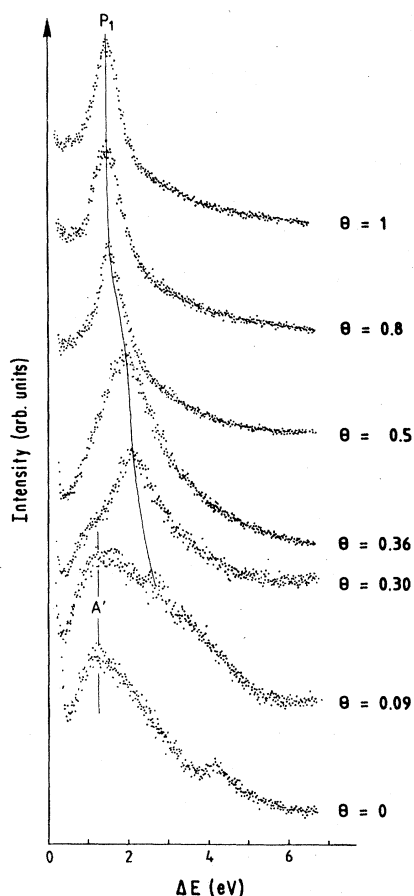


FIG. 11. Cs/W(100). EELS spectra for increasing Cs coverage Θ . The energy of the incident electron beam (with incident angle $=45^\circ$) is $E_0=45$ eV.

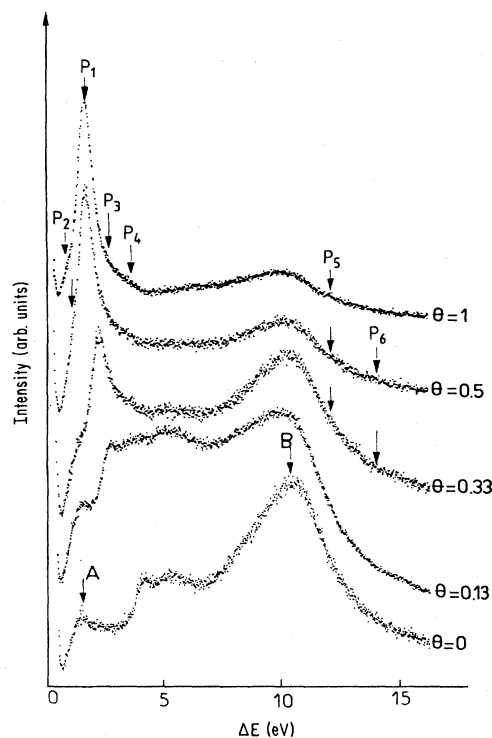


FIG. 12. Cs/Mo(100). EELS spectra for increasing Cs coverage. The energy of the incident electron beam (with incident angle $=48^\circ$) is $E_0=125$ eV (after Ref. 13).

Mo substrate). This structure is attributed to the reconstruction of the substrate. Two further states are observed: (i) At a Cs coverage of $\Theta=0.58$ a $p(2 \times 2)$ structure is developed. Above this coverage, two domains are observed in which the $p(2 \times 2)$ structure is contracted in one of the $[110]$ directions. (ii) At the completed Cs monolayer (denoted in this paper by $\Theta=1$) a compact

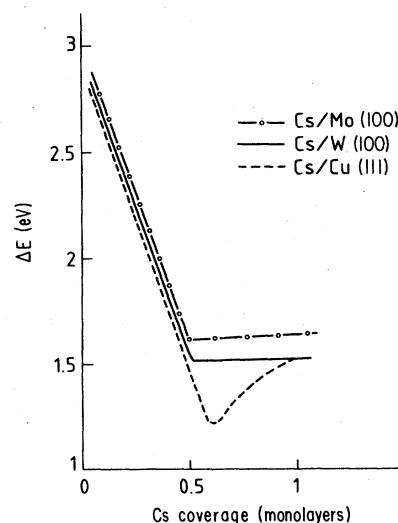


FIG. 13. EELS. Displacement for main loss peak P_1 with increasing Cs coverage for the W(100), Mo(100), and Cu(111) surfaces. [The results for Cu(111) are taken from Ref. 31.]

hexagonal structure is observed, present in two unequally populated domains. At this stage, the coverage with respect to the substrate is 0.43. From these studies^{14,15} it is concluded that a $(\sqrt{2} \times \sqrt{2})R45^\circ$ substrate mesh with the $p2mg$ space group exists on the surface. This structure is present in two domains, one being selectively formed. The intensity of the reflections due to this structure has a twofold symmetry and is attributed to a reconstruction of the Mo substrate which probably differs from that at low coverage where a fourfold symmetry is observed. This second reconstruction¹⁴ appears above 0.7 monolayer of Cs.

V. DISCUSSION AND INTERPRETATION

A. Monolayer coverage

One of the most striking results of the all-electron LDF calculations for a monolayer of Cs adsorbed on W(100) and Mo(100) is the fact that in both cases the high-lying SS at $\bar{\Gamma}$ is shifted by about 1 eV toward larger binding energies (cf. Fig. 14). The charge density plots of the high-lying SS at $\bar{\Gamma}$ for the clean (Fig. 15) and cesiated (Fig. 16) Mo(100) and W(100) surfaces reveal the electronic origin of these shifts: these d_{z^2} -like SS's, which project far out into the vacuum, form a polarized covalent bond with the (Cs-6s)-derived states thus leading to the formation of bonding states of lower one-particle energy than that of each partner. (The corresponding antibonding state is an unbound continuum state located above the vacuum zero of the system.) Surprisingly, the Mo(100) and the W(100) SS's show amazing similarity. It may thus be concluded that either (i) the pronounced attenuation observed for the high-lying Mo(100) SS (cf. Fig. 7), which is so different from the behavior found for the corresponding W(100) SS (cf. Fig. 1), cannot be attributed to a simple initial state effect or (ii) it is due to differences in the adsorption geometry (e.g., height).

From the intensity $I(E_1)$, the d character in the Cs-6s/W-5d hybridization process may be estimated.

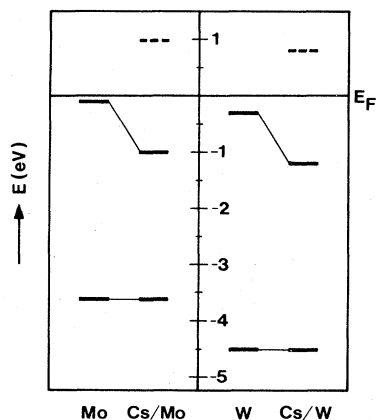


FIG. 14. All-electron LDF FLAPW eigenvalues of the high- and low-lying surface states at $\bar{\Gamma}$ for the clean and cesiated Mo(100) and W(100) surfaces. The broken lines indicate states of predominantly Cs- p character.

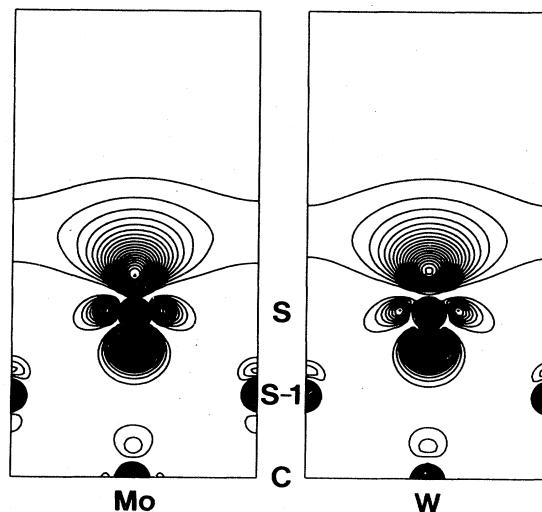


FIG. 15. All-electron LDF FLAPW charge densities [in units of 10^{-3} electrons/(a.u.)³] of the high-lying SS's at $\bar{\Gamma}$ for Mo(100) and W(100).

This intensity is proportional to $(\alpha |s| + \beta |d|)^2$ (α and β being the coefficient of s and d electrons with $\alpha^2 + \beta^2 = 1$). As coverage is increased from 0 to 0.6 monolayers, $I(E_1)$ decreases to 65% of its initial value on the clean surface, then remains constant with increasing Cs coverage (cf. Fig. 17). Due to the fact that these ARUPS experiments were performed at 78 eV, which is not favorable for observing the Cs 6s level (the highest cross section for s levels are obtained for photons with energies of a few electron volts^{7,73}), we can estimate the proportion of d character in the hybridized orbital s, d as $\beta^2 = [I(E_1) \text{ at } 1 \text{ monolayer of Cs} / I(E_1) \text{ on clean W}] = 65/100$; thus $\beta = 80\%$ of d character between 0.6 to 1 monolayer of cesium. Thus the d character of E_1 is reduced by 20% as coverage increases from 0 to 0.6 monolayer and then

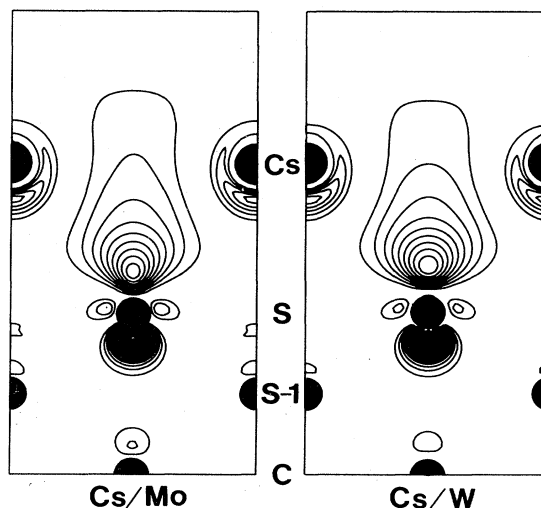


FIG. 16. All-electron LDF FLAPW charge densities of the high-lying SS's at $\bar{\Gamma}$ for cesiated Mo(100) and W(100). The same normalization and units are used as in Fig. 15.

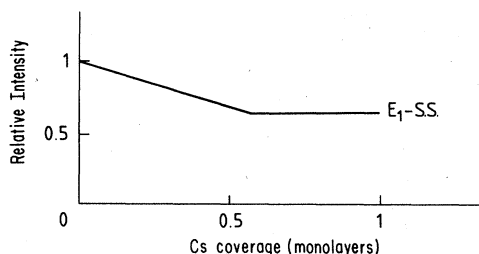


FIG. 17. Relative intensity of the E_1 tungsten surface state peak versus Cs coverage.

remains constant up to 1 Cs monolayer (Fig. 17).

Interestingly, the energy of the low-lying SS at $\bar{\Gamma}$ (cf. Fig. 14) is not affected by cesiation. This fact is readily explained by an inspection of the charge density of this state:^{17,74} this state is mainly localized between the surface and subsurface layer and projects only slightly out into the vacuum region. As a result, its interaction with an adsorbate such as Cs is rather small.

It was suggested in previous studies^{12,13} that the main energy-loss peak P_1 (cf. Figs. 11 and 12) results from interband transitions. Further support for this assumption was obtained from EELS measurements on the coadsorption of oxygen and cesium on Mo(100) (Ref. 62) and W(100).⁷⁵ The interpretation was deduced from a comparison of the loss spectra for Cs on W(100) and Mo(100) with those observed for Cs on Cu(111) (Ref. 31) (Fig. 13) where the relationship between the energy loss and the coverage above the minimum supports the assumption of a surface-plasmon excitation of free electrons. Earlier, MacRae *et al.*³² interpreted their EELS results for Cs on W(100) by assuming surface-plasmon excitations. This picture was supported by the observation that for Cs coverages above one monolayer, the surface-plasmon energy of pure Cs is approached. MacRae *et al.*³² adopted the simple picture^{43,44} that at low coverages, Cs is adsorbed as an ion, becoming atomic-like near half-monolayer coverage and metallic for $\Theta=0.8$ to 1 monolayer. However, MacRae *et al.*³² used a retarding field analyzer with low resolution and they did not observe changes in the energy of the main loss peak for coverages smaller than half a monolayer of Cs. Furthermore, earlier theories such as that of Muscat and News^{51,76} assumed that the interactions between the Cs electrons and the d electrons of the transition metal are negligible and that interactions should occur only with the more delocalized s and p electrons. As a result, one should expect delocalized or free electrons on the W(100) surface, similar to that existing for Cs adsorbed on Cu(111).³¹

A different point of view arises from our all-electron LDF calculations for Cs on W(100) (Ref. 16) and Mo(100).¹⁷ These calculations reveal that the (Cs-6s)-derived valence states are strongly hybridized with localized W(d) surface state electrons. Due to this component of localized states, a collective oscillation, if it would exist, would be markedly damped and a correspondingly large linewidth would occur. Since the characteristic loss peaks, P_1 (cf. Figs. 11 and 12) are sharp, the interpretation involving collective oscillations is unlikely to be ade-

quate and an $s \rightarrow p$ interband transition is assumed as explained in the following.

The EELS spectra shown in Figs. 11 and 12 have been obtained in a specular geometry where "vertical" ($\Delta k_{\parallel}=0$) one-electron transitions and $q_{\parallel}=0$ collective modes are observed. Assuming interband transitions, contributions over the entire surface Brillouin zone have to be taken into account. A first orientation can be gained from analysis of the energy-band structure of an unsupported hexagonal Cs monolayer.⁷⁷ There exist a half-filled s band and an unoccupied, predominantly p -like band⁷⁸ about 1.5 eV above the s band. Both bands exhibit an upward dispersion away from $\bar{\Gamma}$ and are fairly parallel over a considerable part of the surface Brillouin zone. Thus, dipole transitions from the s band into the p band can be expected to give rise to rather large intensities. Similarly, the Cs s - and p -like bands in the energy-band structures of Cs monolayers adsorbed on W(100) (Ref. 16) and Mo(100) (Ref. 17) reveal a partly occupied s band and an unoccupied p band, both with an upward dispersion away from $\bar{\Gamma}$. Interestingly, at $\bar{\Gamma}$, the energy difference between the s band (i.e., the hybridized surface state) and the p band as shown in Fig. 14 is about 2 eV, which is very close to the value of 1.9 eV found for the unsupported Cs monolayer (cf. Fig. 2 of Ref. 77). As stated above, in the case of Cs adsorbed on a transition-metal surface such as W(100), the Cs valence states are hybridized with the substrate d states and polarized towards the transition-metal atoms. Thus, the states near -1 eV in Fig. 14 can be viewed as shifted surface states as discussed in the previous sections and, at the same time, as the bottom of the Cs s band. Away from $\bar{\Gamma}$, this Cs s band disperses upward and hybridizes with other substrate states in a rather complicated way. Importantly, because the bottom of the Cs s band is well below the Fermi level, a significant fraction of this band is occupied giving rise to a sufficient intensity in the $s \rightarrow p$ transitions which therefore could account for the principal energy-loss peaks shown in Figs. 11 and 12.

B. Submonolayer coverage

So far, we have restricted our discussion to the monolayer coverage, for which a comparison with theoretical calculations is possible. We now focus on low Cs coverages of the W(100) surface.

The spectra obtained by ARUPS (Figs. 1–10) and EELS (Figs. 11–13) remain essentially constant as the Cs coverage is increased from 0.5 monolayer to a full monolayer. Therefore, no dramatic change in the electronic structure over this coverage range can be inferred (Fig. 18). This finding is somewhat in conflict with the predictions obtained by Wojciechowski⁵⁸ who concluded from jellium model calculations that at "near monolayer coverage" a transition from an ionic adsorbate state to the metallic state should occur. At low coverages, the model of Wojciechowski⁵⁸ and the description by Levine and Gyftopoulos⁴⁷ are in accordance: Up to about half-monolayer coverage, the adsorbate is mainly ionic with charge transfer to the substrate. Covalent bonding becomes important for coverages larger than half a monolayer. This

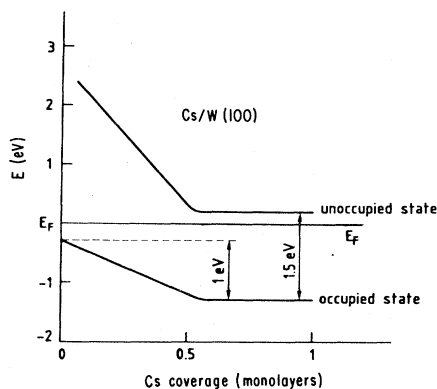


FIG. 18. Cs/W(100). Proposed initial and final state of P_1 interband transition versus cesium coverage between 0 and 1 monolayer.

picture for the high-coverage limit is consistent with the all-electron LDF results.

For low coverages, it is believed that the EELS peaks of several systems result from transitions from a substrate state into an unoccupied resonance state.⁵⁹ In the framework of a simplified quantum-mechanical description of alkali adsorption,^{49,50,58} the drop in the energy loss with increasing coverage is thought to be related to depolarization effects as discussed by Gurney⁴⁸ and Schulte *et al.*⁶⁰

We have shown for Cs on W(100) and on Mo(100), that an apparent continuity seems to exist for both the occupied and unoccupied states up to a half-monolayer coverage (Fig. 18) and that the hybridization between the Cs(6s) and the W(*d*) SS electrons occurs all along the coverage range from 0 to 1 monolayer. This means that the bonding is presumably covalent even at low coverage. Is this conclusion in contradiction with the experimental results in favor of ions at low coverage? First, the observation of an ionic desorption is not directly related to a surface ionization. This was already emphasized by Gurney⁴⁸ and Gomer.⁷⁹ Furthermore, the chemical shift experienced by the core-level electrons, for example, Cs on Cu(111) (Ref. 31) or on Ni(100),²⁹ generally attributed to a strong ionic character at low coverage, may also be the result of the changes in the surface potential,⁸⁰ or to changes in the height of the adatom.

We suggest the following picture to describe the interactions between Cs adsorbates and transition-metal surfaces such as W(100). Due to the extended nature of the Cs 6s orbitals, they interact with localized SS's residing on several neighboring W atoms. With an increased number of Cs atoms, cooperative effects are induced on the W surface which are seen (i) in the reconstruction at low coverage where the induced $c(2 \times 2)$ structure of the substrate has its maximum at a Cs coverage of approximately 0.2 monolayer (0.1 referred to the W surface atom) and (ii) in the occurrence of a single, sharp photoemission peak from hybridized Cs(*s*)-W(*d*) states at low coverages; if Cs would interact with only a few substrate W atoms, two peaks (or one markedly broadened peak) would be observed—one from the "clean" W(*d*) SS and one from the hybridized SS. Cooperative effects through the con-

duction electrons are usually invoked to account for interactions between adatoms.⁸¹ When the Cs coverage is increased, the interaction tends to be more localized on the neighbor atoms due to the Coulomb repulsion of the charge near each W atom. At half-monolayer coverage this localization is fully realized and the final covalent character is reached. However, a change of polarization of the electrons involved must occur in order to reduce the dipole moment, associated with each Cs atom, by a factor of 2 as the coverage is increased from half-monolayer to the full monolayer.

C. Additional spectral features

In the photoemission spectra for Cs on W(100) (Figs. 1–3), a peak E_3 occurs at 2.4 eV below the Fermi energy at a Cs coverage of $\Theta=0.57$ (Fig. 4) and is shifted to 2.6 eV at $\Theta=1$. In this energy range, the clean W(100) surface⁷⁴ does not show states at $\bar{\Gamma}$. A possible origin of the observed E_3 state may be an umklapp process. This effect is known⁸² to be responsible for the appearance of new peaks at \bar{M} when the clean W(100) $p(1 \times 1)$ surface reconstructs into a $(\sqrt{2} \times \sqrt{2})R45^\circ$ structure by cooling below 300 K. When Cs is adsorbed on W(100) (Ref. 18) and on Mo(100),¹⁵ a $c(2 \times 2)$ structure [$(\sqrt{2} \times \sqrt{2})R45^\circ$] is observed at low coverages ($\Theta < 0.22$), which is interpreted¹⁴ in both cases as being due to an adsorbate-induced reconstruction of the substrate. Furthermore, at high Cs coverage, a different adsorbate induced $c(2 \times 2)$ reconstruction of the Mo(100) substrate has been suggested¹⁴ and a similar situation might be present for W(100). Thus, the peak E_3 in the Cs/W(100) spectrum (Fig. 1) could be due to an umklapp process which maps states at 2.6 eV,⁷⁴ from \bar{M} onto $\bar{\Gamma}$. Very recently, we have performed ARUPS experiments⁸³ for this system at the symmetry points $\bar{\Gamma}$ and \bar{M} using a photon energy of $h\nu = 16.85$ eV, which further illustrate this effect. Interestingly, E_3 only occurs at high Cs coverages. The low-lying SS of the W(100) surface⁸⁴ is observed using a photon energy of 65 eV for a Cs coverage of 0.8 monolayer (Fig. 3) with the same binding energy as on the clean surface. At higher photon energies this peak is overlapped by the bulk feature E_5 . Remarkably, the cesium $5p_{3/2}$ and $5p_{1/2}$ semicore level peaks, E_6 and E_7 retain the same binding energies for all Cs coverages.

VI. SUMMARY AND CONCLUSIONS

The adsorption of Cs on the (100) surfaces of W, Mo, and Ta was studied by angle-resolved ultraviolet photoemission spectroscopy (ARUPS), electron-energy-loss spectroscopy (EELS) and auxiliary low-energy electron diffraction (LEED) measurements. For the W(100) and Mo(100) surfaces, the characteristic high-lying SS's are shifted by 1.0 and 0.9 eV, respectively, to larger binding energies as Cs coverage is increased from 0 to 0.6 monolayer. After these initial shifts, the energies of these states remain constant up to full monolayer coverage. These experimental results are in excellent agreement with all-electron local-density-functional calculations for Cs overlayers on W(100) and on Mo(100), performed for the domain of full monolayer coverage. The theoretical inves-

tigations explain the energy shift of the surface state by the formation of a polarized covalent bond between the (Cs-6s)-derived valence states and the W(*d*) substrate surface states. A similar, slightly smaller Cs-induced shift of 0.8 eV is found for the high-lying SS F_1 (Figs. 4 and 5) on the Ta(100) surface. Since recent theoretical investigations of the SS of the clean Ta(100) surface by Krakauer⁷⁰ confirm its similarity with that of the W(100) surface, this leads to an analogous interpretation of the energy shift observed for Cs on Ta(100).

Remarkably, with increased Cs coverage on both the W and Ta surfaces, the Cs 5*p* semicore states do not change their energy with respect to the Fermi level. If one adopts the picture that Cs is more "ionic" at low coverages than at high coverages, this finding clearly demonstrates that the "ionicity" cannot be related simply to core-level shifts. One could instead speculate that there is a second (compensating) contribution to the core-level shift which arises from the change in height of the adsorbate from the substrate.

Surprisingly, deposition of Cs on a Mo(100) surface causes, besides a shift (0.9 eV) of the d_{z^2} -like high-lying SS, a pronounced attenuation of this state. Another effect of the Cs adsorption on Mo(100), not observed on W(100), is the sensitivity of D_3 , the low-lying SS which is shifted by 0.3 eV to smaller binding energies. Furthermore, for increasing Cs coverage the Cs-5*p* semicore states are found to be shifted toward lower binding energies; this is in contrast to the situation observed for the W and Ta(100) surfaces. Assuming the same height (2.9 Å) of the Cs overlayers on the W(100) and Mo(100) surfaces, the FLAPW calculations reveal an amazing similarity between the two isoelectronic transition-metal surfaces. Thus, the observed differences given above could be due to structural (height and reconstruction) differences between the Cs/W(100) and Cs/Mo(100) systems. As a matter of fact, upon deposition of a complete Cs monolayer, the work function is changed by 2.8 eV for W (Ref.

18) and by 3.4 eV for Mo.¹³ Therefore, the height of the Cs atoms should be larger¹⁶ on Mo than on W indicating a slightly weaker bonding between Cs and Mo than between Cs and W. This assumption is further supported by the fact that the adsorption interaction energy for Cs/Mo(110) is smaller than for Cs/W(100).⁸⁵ However, additional investigations are necessary to further clarify this point.

The electron-energy-loss spectra of both the W and Mo(100) surfaces at various Cs coverages between 0 and 1 monolayer reveal a characteristic, sharp loss peak which is shifted to smaller energies with increasing Cs coverage. In Cs on Cu(111), the principal loss peak at high coverages has been interpreted as arising from surface plasmons.^{7,31} We suggest for the W and Mo(100) surfaces, in which localized *d* electrons dominate the density of states at the Fermi energy, that these loss peaks should be interpreted as Cs *s* → *p* interband transitions. Here, in the center of the surface Brillouin zone, the Cs *s* band strongly hybridizes with the high-lying *d*-like surface state.

Finally, the present study clearly demonstrates that the combination of sophisticated experimental techniques and accurate all-electron electronic structure calculations affords a deeper insight into the interaction mechanism of systems such as Cs adsorbed on W, Mo, and Ta surfaces, which are of great technological significance.

ACKNOWLEDGMENTS

We are grateful to Dr. J. Szeftel for stimulating discussions and to Professor H. Krakauer for informing us of his theoretical results on clean Ta(100). Finally, we thank the technical staff of the Laboratoire d'Utilisation du Rayonnement Electromagnétique (LURE) and the Laboratoire de l'Accélérateur Linéaire (LAL) for their assistance. This work was supported in part by the U. S. Office of Naval Research Grant No. N00014-81-K-0438.

*Also at Institut Universitaire de Technologie, Université de Reims-Champagne-Ardenne, F-10026 Troyes, France.

†Permanent address: Institut für Physikalische Chemie, Universität Wien, A-1090 Wien, Austria.

‡Also at Lawrence Livermore National Laboratory, Livermore, CA 94550.

¹C. Noguera, D. Spanjaard, D. Jepsen, Y. Ballu, C. Guillot, J. Lecante, J. Paigne, Y. Petroff, R. Pinchaux, P. Thiry, and R. Cinti, *Phys. Rev. Lett.* **38**, 1171 (1977).

²B. Feuerbacher and R. F. Willis, *Phys. Rev. Lett.* **37**, 446 (1976).

³B. Feuerbacher and N. E. Christensen, *Phys. Rev. B* **10**, 2349 (1974).

⁴S. L. Weng, T. Gustafsson, and W. E. Plummer, *Phys. Rev. Lett.* **44**, 344 (1980).

⁵W. Egelhoff, D. Perry, and T. Linett, *Surf. Sci.* **54**, 670 (1976).

⁶R. L. Billington and T. M. Rhodin, *Phys. Rev. Lett.* **41**, 1602 (1978).

⁷S. A. Lindgren and L. Wallden, *Solid State Commun.* **28**, 282 (1978).

⁸S. A. Lindgren and L. Wallden, *Mater. Sci. Eng.* **42**, 127 (1980).

⁹S. A. Lindgren and L. Wallden, *Chem. Phys. Lett.* **64**, 239 (1979).

¹⁰S. A. Lindgren and L. Wallden, *Solid State Commun.* **34**, 671 (1980).

¹¹J. Paul, S. A. Lindgren, and L. Wallden, *Solid State Commun.* **40**, 395 (1981).

¹²P. Soukiassian, R. Riwan, C. Guillot, J. Lecante, and Y. Borensztein, *Phys. Scr. T* **4**, 110 (1983); P. Soukiassian, R. Riwan, J. Lecante, C. Guillot, and D. Chauveau, *Bull. Am. Phys. Soc.* **28**, 261 (1983).

¹³P. Soukiassian, R. Riwan, and Y. Borensztein, *Solid State Commun.* **44**, 1375 (1982).

¹⁴R. Riwan, P. Soukiassian, S. Zuber, and J. Cousty, *Surf. Sci.* **146**, 382 (1984).

¹⁵R. Riwan, P. Soukiassian, C. Guillot, J. Lecante, and S. Zuber, *Le Vide—Les Couches Minces* **38**, 125 (1983).

¹⁶E. Wimmer, A. J. Freeman, M. Weinert, H. Krakauer, J. R. Hiskes, and A. M. Karo, *Phys. Rev. Lett.* **48**, 1128 (1982); E. Wimmer, A. J. Freeman, J. R. Hiskes, and A. M. Karo, *Phys. Rev. B* **28**, 3074 (1983).

¹⁷S. R. Chubb, E. Wimmer, A. J. Freeman, J. R. Hiskes, and A. M. Karo (unpublished).

- ¹⁸J. L. Desplat, Thèse de Doctorat d'Etat, Université de Paris—Sud, 1974; C. A. Papageorgopoulos and J. M. Chen, *Surf. Sci.* **39**, 283 (1973); V. B. Voronin, A. G. Naumovets and A. G. Fedorus, *Pis'ma Zh. Eksp. Teor. Fiz.* **15**, 523 (1972) [*JETP Lett.* **15**, 370 (1972)].
- ¹⁹A. G. Fedorus and A. G. Naumovets, *Surf. Sci.* **21**, 426 (1970).
- ²⁰S. Andersson and U. Jostell, *Solid State Commun.* **13**, 829 (1973).
- ²¹E. L. Garfunkel and G. A. Somorjai, *Surf. Sci.* **115**, 441 (1981).
- ²²J. O. Porteus, *Surf. Sci.* **41**, 515 (1974).
- ²³S. A. Lindgren, L. Wallden, J. Rundgren, P. Westin, and J. Neve, *Phys. Rev. B* **28**, 6707 (1983).
- ²⁴C. A. Papageorgopoulos, *Phys. Rev. B* **25**, 3740 (1982); J. Cousty, R. Riwan, and P. Soukiassian, *Surf. Sci.* (to be published).
- ²⁵K. Müller, H. Endriss, and K. Heinz, *Appl. Surf. Sci.* **11/12**, 625 (1982).
- ²⁶S. Andersson and J. B. Pendry, *J. Phys. C* **6**, 601 (1973); G. P. Williams, F. Cerrina, I. T. McGovern and G. J. Lapeyre, *Solid State Commun.* **31**, 15 (1979).
- ²⁷B. E. Hayden, K. C. Prince, P. J. Davie, G. Paolucci, and A. G. Bradshaw, *Solid State Commun.* **48**, 325 (1983).
- ²⁸U. Jostell, *Surf. Sci.* **82**, 333 (1979).
- ²⁹L. Surnev, G. Blisnakov, and M. Kiskinova, *Solid State Commun.* **37**, 87 (1981).
- ³⁰S. Andersson and U. Jostell, *Faraday Discuss. Chem. Soc.* **60**, 255 (1975).
- ³¹S. A. Lindgren and L. Wallden, *Phys. Rev. B* **22**, 5967 (1980).
- ³²A. U. MacRae, K. Müller, J. J. Lander, and J. Morrison, *Surf. Sci.* **15**, 483 (1969); A. U. MacRae, K. Müller, J. Lander, and J. C. Phillips, *Phys. Rev. Lett.* **22**, 1048 (1969).
- ³³S. Thomas and T. W. Haas, *J. Vac. Sci. Technol.* **10**, 218 (1973).
- ³⁴J. W. Gadzuk, *Phys. Rev. B* **13**, 1267 (1970).
- ³⁵N. Ghai, E. M. Economou, and M. H. Cohen, *Phys. Rev. Lett.* **24**, 61 (1971).
- ³⁶D. M. Newns, *Phys. Lett.* **38**, 341 (1972).
- ³⁷S. Andersson and U. Jostell, *Surf. Sci.* **46**, 625 (1974).
- ³⁸W. Schröder and J. Hölzl, *Solid State Commun.* **24**, 777 (1977).
- ³⁹Kh. I. Lakh and Z. V. Stasyuk, *Fiz. Tverd. Tela (Leningrad)* **20**, 1989 (1978) [*Sov. Phys.—Solid State* **20**, 1149 (1978)].
- ⁴⁰G. Broden and H. P. Bonzel, *Surf. Sci.* **84**, 106 (1979).
- ⁴¹A. Faldt, *Surf. Sci.* **114**, 311 (1982).
- ⁴²G. Pirug, H. P. Bonzel, and G. Broden, *Surf. Sci.* **122**, 1 (1982).
- ⁴³I. Langmuir, *J. Am. Chem. Soc.* **54**, 2788 (1932).
- ⁴⁴I. Langmuir, *Phys. Rev.* **43**, 224 (1933).
- ⁴⁵J. Topping, *Proc. R. Soc. London, Ser. A* **114**, 67 (1927).
- ⁴⁶J. A. Desplat and C. A. Papageorgopoulos, *Surf. Sci.* **92**, 97 (1980).
- ⁴⁷J. D. Levine and E. P. Gyftopoulos, *Surf. Sci.* **1**, 171 (1964).
- ⁴⁸R. W. Gurney, *Phys. Rev.* **47**, 479 (1935).
- ⁴⁹A. J. Bennett and L. M. Falicov, *Phys. Rev.* **151**, 512 (1966).
- ⁵⁰J. W. Gadzuk, *Surf. Sci.* **6**, 133 (1967).
- ⁵¹J. P. Muscat and D. M. Newns, *Surf. Sci.* **74**, 355 (1978).
- ⁵²J. W. Gadzuk, J. K. Hartman, and T. N. Rhodin, *Phys. Rev. B* **4**, 241 (1971).
- ⁵³B. Rasser and M. Remy, *Surf. Sci.* **93**, 223 (1980).
- ⁵⁴O. M. Braun, L. G. Il'chenko, and E. A. Pashitshii, *Fiz. Tverd. Tela (Leningrad)* **22**, 1649 (1980) [*Sov. Phys.—Solid State* **22**, 963 (1980)].
- ⁵⁵P. Hohenberg and W. Kohn, *Phys. Rev.* **136**, B864 (1964); W. Kohn and L. J. Sham, *ibid.* **140**, A1133 (1965).
- ⁵⁶N. D. Lang, in *Solid State Physics: Advances in Research and Applications*, edited by Frederick Seitz, David Turnbull, and Henry Ehrenreich (Academic, New York, 1973), Vol. 28, p. 225; *Phys. Rev. B* **4**, 4234 (1971).
- ⁵⁷L. M. Khan and S. C. Ying, *Surf. Sci.* **59**, 333 (1976); S. C. Ying, in *Topics in Current Physics, Theory of Chemisorption* (Springer, Berlin, 1980).
- ⁵⁸K. F. Wojciechowski, *Surf. Sci.* **55**, 246 (1976).
- ⁵⁹P. Muscat and D. W. Newns, *Progress in Surf. Sci.* **9**, 1 (1978).
- ⁶⁰J. Schulte and F. Hölzl, in *Solid State Physics*, Vol. 85 of *Springer Tracts in Modern Physics* (Springer, Berlin, 1979), p. 1.
- ⁶¹J. Arlinghaus, J. G. Gay, and J. R. Smith, *Theory of Chemisorption* (Springer, Berlin, 1980), Vol. 72.
- ⁶²P. Soukiassian, R. Riwan, Y. Borensztein, and J. Lecante, *J. Phys. C* **17**, 1761 (1984).
- ⁶³Y. Ballu, *J. Microsc. Spectrosc. Electron. (Paris)* **2**, 231 (1977); Y. Ballu, *Adv. Electron. Electron Phys., Suppl.* **13B**, 257 (1980).
- ⁶⁴Y. Ballu, C. Guillot, J. Lecante, J. Paigne, G. Chauvin, P. Thiry, R. Pinchaux, Y. Petroff, and R. Cinti, *J. Microsc. Spectrosc. Electron. (Paris)* **1**, 165 (1976).
- ⁶⁵P. Della Porta, C. Emili, and S. S. Hellier, *IEEE Conference on Tube Techniques*, New York Technical Report No. 18, 1968 (unpublished).
- ⁶⁶J. E. Inglesfield, *Rep. Prog. Phys.* **45**, 223 (1982); J. E. Inglesfield and D. W. Holland, in *The Chemical Physics of Solid Surfaces and Heterogeneous Catalysis*, edited by D. A. King and D. Woodruff (Elsevier, Amsterdam, 1982), Vol. 1, p. 355.
- ⁶⁷E. Wimmer, H. Krakauer, M. Weinert, and A. J. Freeman, *Phys. Rev. B* **24**, 864 (1981), and references therein.
- ⁶⁸D. D. Koelling and B. N. Harmon, *J. Phys. C* **10**, 3107 (1977).
- ⁶⁹P. Roubin and J. Lecante (unpublished).
- ⁷⁰H. Krakauer, *Bull. Am. Phys. Soc.* **28**, 420 (1983), and private communication.
- ⁷¹Y. Ballu, J. Lecante, and H. Rousseau, *Phys. Rev. B* **14**, 3201 (1976).
- ⁷²Y. Ballu, J. Lecante, and D. M. Newns, *Phys. Lett. A* **57**, 159 (1976); J. Lecante, Y. Ballu, and D. M. Newns, *Phys. Rev. Lett.* **38**, 36 (1977).
- ⁷³N. V. Smith and G. B. Fisher, *Phys. Rev. B* **3**, 11 (1971).
- ⁷⁴M. Posternak, H. Krakauer, A. J. Freeman, and D. D. Koelling, *Phys. Rev. B* **21**, 5061 (1980); M. Posternak, H. Krakauer, and A. J. Freeman, *ibid.* **25**, 755 (1982); S. Ohnishi, A. J. Freeman, and E. Wimmer, *ibid.* **29**, 5267 (1984).
- ⁷⁵P. Soukiassian, R. Riwan, and J. Lecante, *Surf. Sci.* (to be published).
- ⁷⁶J. P. Muscat and D. M. Newns, *Surf. Sci.* **84**, 262 (1979).
- ⁷⁷E. Wimmer, *J. Phys. F* **13**, 2313 (1983).
- ⁷⁸The spin-orbit splitting, which for the atomic Cs $6p_{1/2}$ and $6p_{3/2}$ is less than 0.1 eV, should not be of further concern in this context.
- ⁷⁹R. Gomer, in *Solid State Physics: Advances in Research and Applications*, Ref. 56, Vol. 28, p. 224.
- ⁸⁰R. Richter and J. W. Wilkins, *J. Vac. Sci. Technol. A* **1**, 1089 (1983); S. L. Weng, Ph.D. thesis, University of Pennsylvania, 1978 (unpublished).
- ⁸¹J. Koutecky, *Surf. Sci.* **1**, 280 (1964); T. B. Grimley, *J. Phys. C* **6**, 868 (1973).
- ⁸²J. C. Campuzano, D. King, C. Somerton, and J. Inglesfield, *Phys. Rev. Lett.* **45**, 1649 (1980); J. C. Campuzano, J. Ingles-

- field, D. A. King, and C. Somerton, *J. Phys. C* **14**, 3099 (1981).
- ⁸³J. Cousty, R. Riwan, P. Soukiassian, and F. Mila (unpublished).
- ⁸⁴S. L. Weng, *Phys. Rev. Lett.* **38**, 434 (1977); S. L. Weng, T. Gustafsson, and E. W. Plummer, *ibid.* **39**, 829 (1977); S. L. Weng, E. W. Plummer, and T. Gustafsson, *Phys. Rev. B* **18**, 1718 (1978); S. L. Weng, Ph.D. thesis, University of Pennsylvania, 1978 (unpublished).
- ⁸⁵I. Ya Dekhtyar, V. I. Silant'ev, N. A. Shevchenko, and L. A. Narinskaya, *Ukr. Fiz. Zh. (Russ. Ed.)* **21**, 500 (1976).